

ChemComm

Accepted Manuscript



This is an *Accepted Manuscript*, which has been through the Royal Society of Chemistry peer review process and has been accepted for publication.

Accepted Manuscripts are published online shortly after acceptance, before technical editing, formatting and proof reading. Using this free service, authors can make their results available to the community, in citable form, before we publish the edited article. We will replace this *Accepted Manuscript* with the edited and formatted *Advance Article* as soon as it is available.

You can find more information about *Accepted Manuscripts* in the [Information for Authors](#).

Please note that technical editing may introduce minor changes to the text and/or graphics, which may alter content. The journal's standard [Terms & Conditions](#) and the [Ethical guidelines](#) still apply. In no event shall the Royal Society of Chemistry be held responsible for any errors or omissions in this *Accepted Manuscript* or any consequences arising from the use of any information it contains.

COMMUNICATION

Si/MnOOH composite with superior lithium storage property

Cite this: DOI: 10.1039/x0xx00000x

Hai Zhong^{a,b}, Yanbo Yang^a, Fei Ding^b, Donghai Wang^c, Yunhong Zhou^a, Hui Zhan^{a,*}

Received

Accepted

DOI: 10.1039/x0xx00000x

www.rsc.org/

The Si/MnOOH composite electrode gives very stable cycling and excellent rate capability, such as 1200 mAh g⁻¹ at 12 A g⁻¹, and 700 mAh g⁻¹ at 20 A g⁻¹. The γ -MnOOH component significantly promotes the alloying/de-alloying reaction between Si and lithium.

High energy/power density Li-ion batteries have been pursued since the commercialization of Graphite/LiCoO₂ LiBs, among all the cathode/anode combinations, LiBs with Si anode attracts more attention due to its potential high energy density. Nowadays, silicon have triggered much efforts due to the largest theoretical capacity (Li₂₂Si₅, ~4200 mAh g⁻¹), and relatively lower electrochemical alloy/de-alloy reaction voltage (~0.4 V vs. Li/Li⁺).¹ However, the repeated large volume changes during Li insertion and extraction can lead to electrode failure.² The failure mechanism is believed to involve the particle pulverization, and the electric contact deterioration which will finally cause the electrode disintegration and the rapid capacity fading.³ Recent researches also prove that the solid-electrolyte interphase (SEI) degradation is another reason for the Si anode failure.^{4,5} A number of strategies have been implemented to suppress the volume change and enhance or maintain the electric contact between silicon and the conductive agent. Examples typically are Si or Si/C composite with specially designed architecture, such as silicon nanowires, silicon nanorods, porous silicon and York-shell silicon/C composite,⁶⁻⁹ and they present the expected capacity performance and cycling stability. However, the relatively complicated multi-step synthesis and very fluffy, insufficiently compressible product powder brings the concerns on cost and the electrode fabrication. Except the special material processing or special architecture design, binder optimization or SEI additive has also been proposed to enhance the property of Si anode, and Carboxymethylcellulose (CMC) or Alginate binder and Fluoroethylene carbonate (FEC) additive are now widely used in the researches on Si anode.¹⁰⁻¹²

Though many composites with good property have been successfully synthesized, most of them use carbon or conductive polymer to enhance the electrical contact or buffer the volume expansion. Here we report a new Si/MnOOH composite which shows greatly improved Li-ion storage performance. Hydrothermally prepared γ -MnOOH^{13,14} was ball milled with silicon to form

Si/MnOOH composite. The obtained Si/MnOOH composite exhibits an initial charge capacity of 3058 mAh g⁻¹ at the current of 0.1 A g⁻¹ between 1.5 and 0.01 V. An excellent rate capability has been achieved by the composite electrode, it shows 1200 mAh g⁻¹ capacity at 12 A g⁻¹ and 700 mAh g⁻¹ at 20 A g⁻¹. In addition, Si/MnOOH composite presents a very stable cycling with more than 1000 mAh g⁻¹ after 1500 cycles. The superior electro-activity toward lithium of Si/MnOOH composite should be attributed to γ -MnOOH which has some "catalyzing effect" on the alloying/de-alloying reaction between lithium and silicon.¹⁵

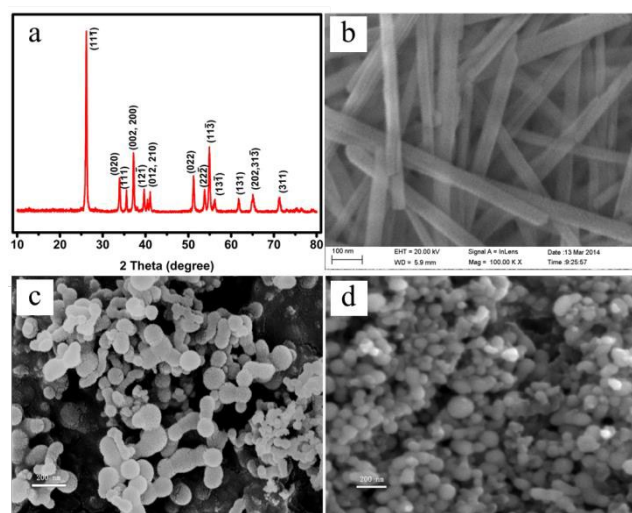


Fig. 1 (a) XRD pattern of γ -MnOOH; (b) SEM image of γ -MnOOH synthesized by the hydrothermal method; (c) SEM image of silicon powder; (d) SEM image of Si/MnOOH composite.

The XRD pattern of the hydrothermally synthesized γ -MnOOH is shown in Fig. 1a. It well agreed with the literature data (manganite, space group P21/c(14), JCPDS 41-1379) and all of the diffraction peaks could be indexed by a monoclinic phase. The sharp peaks indicated good crystallinity and the very notable (111) diffraction line suggested a preferred orientation of the product which could be

further evidenced in SEM observation. Scanning electron microscopy (SEM) (Fig. 1b) image revealed that the as-synthesized γ -MnOOH was one-dimensional (1D) nano-material, and was composed of the nano-rods with an average diameter of 40 nm. The SEM images of silicon and the composite powder are shown in Fig. 1c and 1d respectively. Bare Si had spherical particle with the diameter of about 100 nm, slight particle agglomeration could be observed. After the high-energy ball-milling with γ -MnOOH, the spherical morphology was mostly reserved in Si/MnOOH and the average particle size did not change much.

To better analyze the electrochemical activity of Si/MnOOH composite, γ -MnOOH alone was first examined in 1 M LiPF₆/EC+DMC electrolyte. After the low efficiency in the 1st cycle, the coulombic efficiency increased gradually until finally stabilized at around 98% (Fig. S1a in ESI†). In addition, the voltage profile (Fig. S1b in ESI†) and the differential dQ/dV plot (Fig. S1c in ESI†) indicated that after the 1st charge/discharge, the electrochemical behavior of γ -MnOOH was quite similar to MnO except a higher reducing voltage.^{16,17} The result suggests that the redox reaction of γ -MnOOH should follow the route of γ -MnOOH + Li⁺ + e⁻ ↔ MnO + LiOH and MnO + 2Li⁺ + 2e⁻ ↔ Mn + Li₂O, thus γ -MnOOH phase first decomposes into MnO and then a conversion reaction of MnO happens. The higher reducing voltage of MnOOH than MnO may further imply the “catalyzing effect” of LiOH, and similar observation has also been obtained on Ni(OH)₂ anode which showed a higher reducing voltage than NiO.^{18,19}

The effect of γ -MnOOH on Si anode was investigated by electrochemical tests. Si/MnOOH composite with different γ -MnOOH content was obtained by ball-milling. The optimum ratio of Si/MnOOH=55:5 was chosen according to the result in Fig. S2 (in ESI†). Elemental mapping in Fig. S3 b-d (in ESI†) showed the uniform distribution of Mn and O along with silicon in Si/MnOOH composite (Fig. S3a in ESI†), confirming the homogeneous disperse of γ -MnOOH in Si powder.

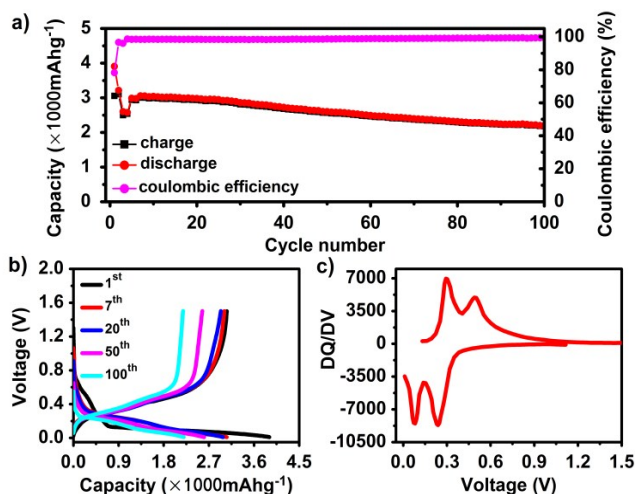


Fig. 2 (a) Plot of charge/discharge capacity and coulombic efficiency vs. cycles of Si/MnOOH electrode (0.1 A g⁻¹ in the first two cycles, 2 A g⁻¹ in the rest of cycles); (b) Voltage profiles of Si/MnOOH electrode at different cycles; (c) DQ/dV curve of Si/MnOOH electrode at the 7th cycle.

The electrochemical property of Si/MnOOH composite was evaluated by galvanostatic charge-discharge tests, and the capacity is based on the mass of the composite. Fig. 2a displays the cycling stability of Si/MnOOH electrode. Two “formation” charging/dis-

charging with a low current of 0.1 A g⁻¹ was applied, and then the current of 2 A g⁻¹ was adopted in the subsequent cycles. In the 1st cycle, the discharge and charge capacity was 3907 mAh g⁻¹ and 3058 mAh g⁻¹ respectively, corresponding to the coulombic efficiency of 78.3%. With the current increasing to 2 A g⁻¹, the capacity dropped to 2605/2501 mAh g⁻¹ in the 3rd cycle, but recovered to above 3000 mAh g⁻¹ in the 7th cycle. Similar observation was obtained previously on nano-Si.²⁰ Actually, the formation process to completely activate the electrode material has been widely reported on the electrode with a mesoporous/microporous structure and is explained by the gradual electrolyte impregnation into the electrode.^{21,22} After the initial formation cycles, a maximum capacity of 3056/3007 mAh g⁻¹ was reached at the 7th cycle. Very slow capacity decay happened in the subsequent cycles, after 100 cycles, the electrode could release near 2200 mAh g⁻¹ capacity. Even after 1500 cycles, the capacity was still above 1200 mAh g⁻¹ (Fig. S4 in ESI†). The voltage profiles of Si/MnOOH electrode in different cycle is shown in Fig. 2b. We can see that except in the first cycle, the voltage hysteresis between the charge and the discharge plateau gradually increased with cycling but still kept very small within 100 cycles. To better understand the redox process of Si/MnOOH electrode, a differential analysis was conducted on the 7th charge/discharge curve and the result is displayed in Fig. 2c. The alloying/de-alloying of lithium with Si led to two pair of redox peaks at 0.29/0.08 V and 0.48/0.24 V vs. Li/Li⁺. The result is consistent with previous report on Si and should be attributed to the phase transformation between different amorphous Li_xSi.²³ The small voltage segregation between the oxidizing and reducing branch indicated the good reaction reversibility of Si/MnOOH. However, we could not unambiguously discern the redox peak of γ -MnOOH, and the reasons may be the low proportion of γ -MnOOH in the composite electrode or the redox peaks of γ -MnOOH being covered by those of silicon.

Si/MnOOH electrode exhibited an excellent rate capability. In Fig. 3a, at the low current of 0.1 A g⁻¹, the capacity of Si/MnOOH was just slightly higher than Si electrode, such as 3100 mAh g⁻¹ to 2900 mAh g⁻¹; however, when the current increased to 1 A g⁻¹, more than 2800 mAh g⁻¹ capacity was obtained on Si/MnOOH while barely 2000 mAh g⁻¹ on Si. The capacity difference was more notable when the current increased further. The pristine Si anode almost failed at the current of 8 A g⁻¹, and Si/MnOOH electrode still could be discharged to around 1600 mAh g⁻¹. The voltage-capacity profile in Fig. 3b more clearly shows the capacity/energy advantage of Si/MnOOH over Si. For Si/MnOOH, the capacity only dropped from 3197 mAh g⁻¹ at 0.1 A g⁻¹ to 2800 mAh g⁻¹ at 1 A g⁻¹, while the voltage gap between charging and discharging kept almost constant. Even at the current of 12 A g⁻¹, a decent capacity around 1200 mAh g⁻¹ was delivered. It is worth noted that Si/MnOOH electrode presented an appreciable capacity of 700 mAh g⁻¹ at 20 A g⁻¹. To our knowledge, such capacity has seldom been reported on silicon-based material in the ultrafast charge/discharge mode. Actually, even on a “super thick” Si/MnOOH electrode (mass loading is 3 mg cm⁻², the ratio of active material: acetylene black: PAA binder is 6:3:1, specific area capacity at 1 A g⁻¹ is 4.5 mAh cm⁻²), the improvement in rate capability is still very significant (Fig. S5 in ESI†), however, the stable cycling will require more work on binder because of much more serious electrode peeling during electrode fabrication and electrode cycling. As the performance is obtained on Si/MnOOH composite prepared by a simple ball-milling, further enhanced capacity/energy performance can be reasonably expected if architecture design or component optimization can be involved.

The AC Impedance comparison supplies some clues for the better electrochemical performance of Si/MnOOH than Si (Fig. 3c). After 100 cycles, impedance spectra were collected on both electrodes. They all showed two semicircles in the high and high-to-medium

frequency range, which represents Li^+ diffusion through the SEI and charge-transfer reaction, and can be indexed by R_{SEI} and R_{ct} respectively according to the equivalent circuit diagram. The low-frequency Warburg slope represents the semi-infinite diffusion of lithium-ion in the electrodes.²⁴ Comparing the impedance diagrams, we can see that Si/MnOOH electrode had smaller semicircles than Si electrode in the high-frequency and medium-frequency region, suggesting the smaller R_{SEI} and R_{ct} of Si/MnOOH electrode than Si electrode. The fitted data in Table S1 (in ESI†) indicates that the R_{ct} value of Si/MnOOH is much smaller than of Si electrode, and the result reveals the much better reaction kinetics of Si/MnOOH than Si. The very close Warburg factor (σ) of Si and Si/MnOOH electrode suggests the similar Li^+ diffusion coefficient of these two electrodes,²⁵ and it is reasonable because Si and Si/MnOOH has very similar particle size and the essentially same structure (the very low proportion of MnOOH in Si/MnOOH composite will not significantly affect the structure of bulk material). We think the impedance results explain the excellent cycling stability and rate capability of Si/MnOOH composite and may imply the “catalyzing” effect of γ -MnOOH on the alloy/de-alloy reaction of Si anode, more works is still in progress on this point.

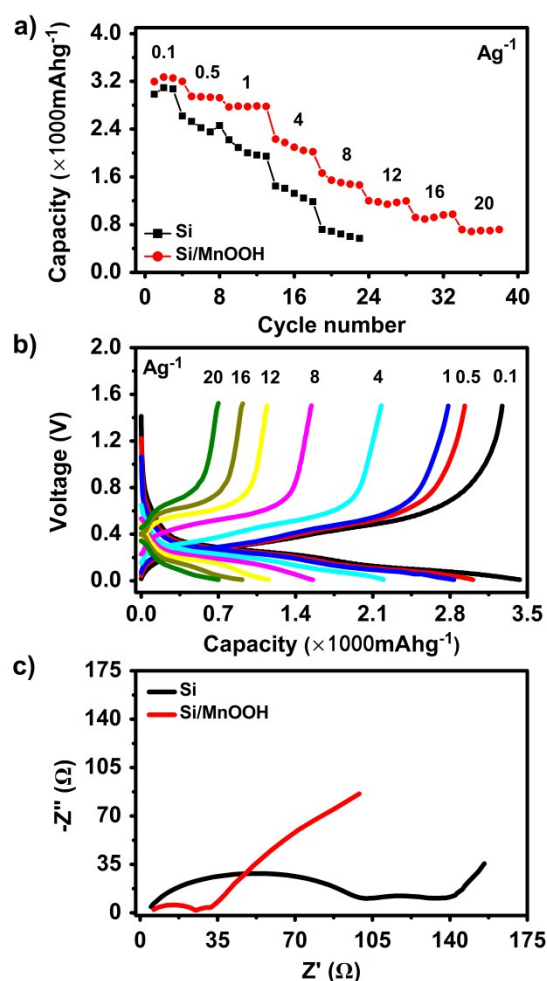


Fig. 3 (a) Discharging capacity vs. cycle number for bare silicon electrode and Si/MnOOH electrode at different current density in the voltage range of 0.01–1.5 V; (b) Voltage profiles of bare silicon electrode and Si/MnOOH electrode at the current density of 0.1, 0.5, 1, 4, 8, 12, 16 and 20 A g^{-1} ; (c) AC Impedance of bare silicon electrode and Si/MnOOH electrode after 100 cycles.

Conclusions

In conclusion, nano-rod γ -MnOOH was prepared through a hydrothermal method, and then ball-milled with Si to form Si/MnOOH composite. The as-prepared Si/MnOOH composite showed a high capacity about 3900mAh g^{-1} and very stable cycling. Additionally, the composite exhibited an excellent rate capability, such as 1200mAh g^{-1} at 12A g^{-1} , and 700mAh g^{-1} at 20A g^{-1} . The result supplies a new strategy to enhance the electrochemical performance of Si anode, and the facile preparation offers a new way to obtain mass-producible Si anode material with perfect Li-ion storage property.

Notes and references

^a Department of chemistry, Wuhan University, Hubei, 430072, China.

^b Tianjin Institute of Power Source, Tianjin, 300381, China

^c Department of Mechanical and Nuclear Engineering, The Pennsylvania State University, University Park, Pennsylvania, 16802, United States

* Corresponding Author, E-mail: zhanhui3620@126.com

Authors would express their sincere thanks to the Nature Science Foundation of China (No.21073138, 21273168, 21233004) for the financial support.

† Electronic Supplementary Information (ESI) available: [sample synthesis, experimental condition, electrochemical property of MnOOH and different ratio Si/MnOOH]. See DOI: 10.1039/c000000x/

- J. X. Song, M. J. Zhou, R. Yi, T. Xu, M. L. Gordin, D. H. Tang, Z. X. Yu, M. Regula and D. H. Wang, *Adv. Funct. Mater.*, 2014, **24**, 5904–5910.
- J. H. Ryu, J. W. Kim, Y. E. Sung and S. M. Oh, *Electrochem. Solid-State Lett.*, 2004, **7**, A306–A309.
- X. Yang, Z. Wen, X. Xu, Z. Gu and S. Huang, *Electrochem. Solid-State Lett.*, 2007, **10**, A52–A55.
- M. Y. Nie, D. P. Abraham, Y. J. Chen, A. Bose and B. L. Lucht, *J. Phys. Chem. C*, 2013, **117**, 13403–13412.
- Y. Liu, X. Guo, J. F. Li, Q. L. Lv, T. Y. Ma, W. T. Zhu and X. P. Qiu, *J. Mater. Chem. A*, 2013, **1**, 14075–14079.
- N. Du, X. Fan, J. X. Yu, H. Zhang and D. R. Yang, *Electrochem. Commun.*, 2011, **13**, 1443–1446.
- R. Teki, M. K. Datta, R. Krishnan, T. C. Parker, T. M. Lu, P. N. Kumta and N. Koratkar, *Small*, 2009, **5**, 2236–2242.
- H. Zhong, H. Zhan and Y. H. Zhou, *J. Power Sources*, 2014, **262**, 10–14.
- N. Liu, H. Wu, M. T. McDowell, Y. Yao, C. M. Wang and Y. Cui, *Nano Lett.*, 2012, **12**, 3315–3321.
- J. C. Guo and C. S. Wang, *Chem. Commun.*, 2010, **46**, 1428–1430.
- I. Kovalenko, B. Zdyrko, A. Magasinski, B. Hertzberg, Z. Milicev, R. Burtovyy, I. Luzinov and G. Yushin, *Science*, 2011, **334**, 75–79.
- Y. M. Lin, K. C. Klavetter, P. R. Abel, N. C. Davy, J. L. Snider, A. Heller and C. B. Mullins, *Chem. Commun.*, 2012, **48**, 7268–7270.
- V. M. B. Crisostomo, J. K. Ngala, S. Alia, A. Doble, C. Morein, C. H. Chen, X. F. Shen, S. L. Sui, *Chem. Mater.*, 2007, **19**, 1832–1839.
- G. Tao, K. Frank, N. Reinhard, *Inorg. Chem.*, 2009, **48**, 6242–6250.
- L. L. Zhang, X. B. Zhang, Z. L. Wang, J. J. Xu, D. Xua and L. M. Wang, *Chem. Commun.*, 2012, **48**, 7598–7600.

- 16 Y. Xia, Z. Xiao, X. Dou, H. Huang, X. H. Lu, R. J. Yan, Y. P. Gan, W. J. Zhu, J. P. Tu, W. K. Zhang and X. Y. Tao, *ACS Nano*, 2013, **7**, 7083-7092.
- 17 G. L. Xu, Y.F. Xu, H. Sun, F. Fu, X. M. Zheng, L. Huang, J. T. Li, S. H. Yang and S. G. Sun, *Chem. Commun.*, 2012, **48**, 8502-8504.
- 18 S. B. Ni, X. H. Lv, T. Li, X. L. Yang and L. L. Zhang, *J. Mater. Chem. A*, 2013, **1**, 1544-1547.
- 19 X. H. Huang, J. P. Tu, X. H. Xia, X. L. Wang and J. Y. Xiang, *Electrochem. Commun.*, 2008, **10**, 1288-1290.
- 20 J. C. Guo, A. Sun and C. S. Wang, *Electrochem. Commun.*, 2010, **12**, 981-984.
- 21 L. C. Yang, Q. S. Gao, Y. H. Zhang, Y. Tang and Y. P. Wu, *Electrochem. Commun.*, 2008, **10**, 118-122.
- 22 Y. F. Shi, B. K. Guo, S. A. Corr, Q. H. Shi, Y. S. Hu, K. R. Heier, L. Q. Chen, R. Seshadri and G. D. Stucky, *Nano Lett.*, 2009, **9**, 4215-4220.
- 23 J. Li and J. R. Dahn, *J. Electrochem. Soc.*, 2007, **154**, A156-A161.
- 24 J. Liu and A. Manthiram, *Chem. Mater.*, 2009, **21**, 1695-1707.
- 25 H. Liu, C. Li, H. P. Zhang, L. J. Fu, Y. P. Wu and H. Q. Wu, *J. Power Sources*, 2006, **159**, 717-720.